Journal of Statistical Mechanics: Theory and Experiment
An IOP and SISSA journal

Anomalous scaling behavior in polymer thin film growth by vapor deposition

Seung-Woo Son, Meesoon Ha[1] and Hawoong Jeong

Department of Physics, Institute for the BioCentury, KAIST, Daejeon 305-701, Korea
E-mail: sonswoo@kaist.ac.kr, msha@kaist.ac.kr and hjeong@kaist.ac.kr

Received 13 November 2008
Accepted 17 December 2008
Published 11 February 2009

Online at stacks.iop.org/JSTAT/2009/P02031
doi:10.1088/1742-5468/2009/02/P02031

Abstract. As a first step towards understanding the anomalous kinetic roughening with multifractality found in recent experiments on vapor deposition polymerization (VDP) growth, we study a simple toy model of the VDP growth in a $(1+1)$-dimensional lattice, along with monomer diffusion, polymer nucleation, limited active end bonding, and shadowing effects. Using extensive numerical simulations, we observe that the global roughness exponent is different from the local one. It is argued that such anomalies in VDP growth are attributable to the instability induced by the non-local shadowing effects on active ends of polymers. Varying the ratio of the diffusion coefficient to the deposition rate by means of a cosine flux, we also consider the role of diffusion in kinetic roughening of polymer thin film growth, which is quite different from that for metal or semiconductor film growth. Finally, we suggest a $(2+1)$-dimensional version, which can be directly compared with experimental results.

Keywords: chemical vapor deposition (theory), kinetic roughening (theory), self-affine roughness (theory), thin film deposition (theory)

ArXiv ePrint: 0811.2169

[1] Author to whom any correspondence should be addressed.

1742-5468/09/P02031+13$30.00

Contents

1. Introduction

In the last few years, kinetic roughening of non-equilibrium steady states for the growth of thin films and multilayers has been an issue of considerable interest [1, 2]. This is motivated by the demand for smooth or regularly structured surfaces and interfaces for miniaturized functional films in science and technology. Such interest is explained by the relevance to surface film characterization at the submicron level, and the mechanisms that determine the film morphology and can contribute to achieving better control of the film properties in real applications.

Although lots of theoretical and experimental studies have shown the existence of kinetic roughening and in many cases revealed the occurrence of scaling exponents corresponding to a few universality classes, there is no general picture of kinetic roughening for the growth of polymer thin films. This is because the major efforts have been focused on the growth of metal and semiconductor thin films. Now that the polymer thin films are growing in technological interest, as regards molecular device and microelectronic interconnect use [3], the few such studies are known as pioneering works, where also kinetic roughenings with various scaling behaviors are shown [4]–[6]. Among the many techniques for polymer thin film growth, vapor deposition polymerization (VDP) best describes the process of coating with poly(p-xylylene) (PPX), also known by the trade name Parylene [7], where the monomer from the gas phase condenses on the substrate, reacts to form a high molecular weight substance, as an oligomer, and becomes a part of the polymer. In the present study, we mimic such VDP processes, in terms of a modified MBE-type growth model, discuss kinetic roughening of the polymer thin film growth by vapor deposition, and give a guideline for VDP growth model studies for explaining the experimental data from the growth of polymer thin films.

This paper is organized as follows. In section 2, we describe our model for the VDP growth in a $(1+1)$-dimensional lattice and show the evolution of surface morphologies with and without shadowing effects caused by a cosine flux. In section 3, numerical results

J. Stat. Mech. (2009) P02031

are presented for kinetic roughening with multifractality measuring surface roughness, height difference correlation functions, the density profile, height and step distributions. Finally, we discuss the physical origin of the anomalous scaling behaviors as well as polymer characteristics, and suggest a possible extension of the VDP model to a $(2+1)$-dimensional lattice, to be compared with recent experimental data for PPX-C film growth. We conclude the paper in section 4 with a brief summary and remarks.

2. Model

We mimic the polymer thin film growth by the VDP process in terms of a simple toy model that was proposed by Bowie and Zhao [8], for a $(1+1)$-dimensional lattice with L sites, where we use a periodic boundary condition in a spatial direction, x, and add the coalescence process of polymers to the original model.

During the VDP process, the monomer transport in the vacuum is very similar to the conventional physical vapor deposition (PVD) process, i.e., the molecular beam epitaxy (MBE) process for metals or semiconductors [1]. However, there are quite large differences in the nucleation and growth processes after the monomer is condensed on the substrate or the film surface. In the PVD/MBE process, monomers are stable once they attach to the nearest neighbors of any nucleated sites, so the films get dense and compact as monomer diffusion increases. In contrast, they become stable in the VDP process only when they reach one of two active ends of a polymer chain, and the films get rough as monomer diffusion increases since it occurs along the polymer bodies. Other surface dynamics can also affect the growth differently in the two cases. While surface diffusion, edge diffusion, and step barrier effects are relevant to the PVD/MBE case, intermolecular interaction and chain relaxation are relevant to the VDP case, besides monomer diffusion. Such differences give a distinct dynamic behavior for the VDP film morphology.

Dynamic rules and updates

For simplicity, we omit the chain relaxation in our model and consider only the following five processes (see figure 1):

Deposition. At each step, a monomer is activated into the system with an angle of incidence θ to the vertical direction, which follows the distribution of $\cos(\theta)$, not a collimated flux form. This incidence of monomers with an angle distribution is called a *cosine flux* [9] with the deposition rate F, the number of incident monomers per site for unit time.

Surface diffusion. Before the activated monomers are stabilized, an incident monomer deposited onto the polymer body sides or substrate randomly wanders from one site to another site along the polymer bodies or substrate with diffusion coefficient D at each deposition step, where D is the number of hops per monomer for unit time. The surface growth is controlled by the ratio of the diffusion coefficient to the deposition flux, $G = D/F$. From now on we set $F = 1$ for convenience, such that $G = D$.

Nucleation. When two monomers meet on substrate or polymer bodies, they form a dimer as a polymer seed, i.e., oligomer, which is called *nucleation (initiation)*. In contrast to the MBE growth where atoms can attach to the nearest neighbors of

J. Stat. Mech. (2009) P02031

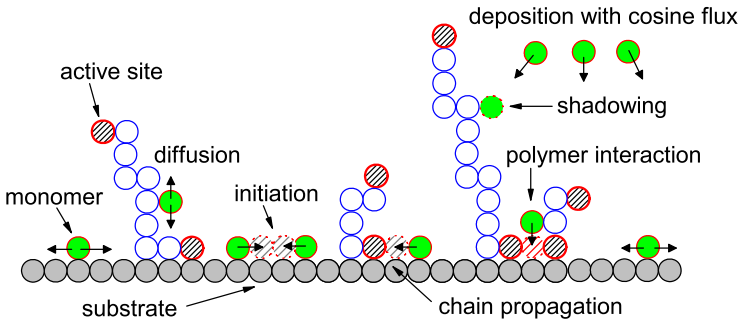

Figure 1. Five dynamics rules are illustrated as solid circles for monomers, open circles with thin lines for polymer bodies, and patterned circles with thick lines for active ends.

the nucleated sites, in the VDP growth the stabilization reaction occurs only at the active ends of a polymer chain, so-called active sites. Such active bonding in the VDP growth is a key ingredient, as well as the cosine flux for monomer deposition.

Propagation. When a monomer reaches one of the active ends of a polymer, it is stabilized as part of the polymer and at the same time it becomes the active end of the polymer. This is called *chain propagation*.

Coalescence. In the process of the chain propagation, it is possible that an active end of a polymer meets that of another polymer. Then two polymers are merged into one long polymer. This process is called *coalescence (polymer interaction)*. It is worthy of note here that, for linear polymers, only the two ends of the chain are active, and are ready for reacting with monomers or other polymers. However, we do not allow a polymer loop. In other words, if one active end of a polymer meets the other side of the active end of itself, the two active ends cannot merge into a stabilized polymer loop and such a try is rejected.

Performing Monte Carlo (MC) simulations for the VDP growth model, we use the random sequential (continuous time) updating method, in terms of the deposition probability of an incident monomer, P_F, and the diffusion probability of an ad-monomer, $P_{\rm D}$, with the definitions $P_F = (FL/DN_{\rm m} + FL)$ and $P_{\rm D} = 1 - P_F = (DN_{\rm m}/DN_{\rm m} + FL)$, respectively. Here $N_{\rm m}$ is the number of ad-monomers and L is the system size. We rewrite the probabilities using the ratio G of the diffusion coefficient D to the deposition rate F, $G = D/F$, and the ad-monomer density $\rho_{\rm m} = N_{\rm m}/L$:

$$P_F = \frac{1}{G\rho_{\rm m} + 1}, \qquad \text{and} \qquad P_{\rm D} = \frac{G\rho_{\rm m}}{G\rho_{\rm m} + 1}.$$

The detailed procedure of our MC simulations is as follows. First, generate a random number, $p \in (0, 1]$. If $p < P_F$, a monomer is deposited on the polymer bodies or substrate from the cosine flux with a randomly chosen angle. Otherwise, an ad-monomer randomly chosen from $N_{\rm m}$ monomers diffuses in a randomly chosen direction. Then, the final surface configuration is governed by the above five VDP processes. The MC time is updated with the unit of a monolayer (ML) after every Lth monomer is deposited.

J. Stat. Mech. (2009) P02031

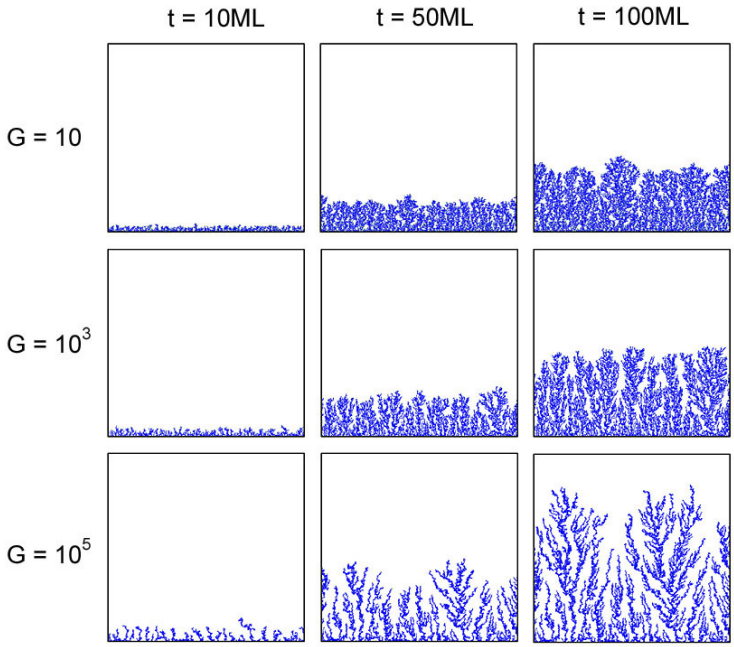

Figure 2. Snapshots of the VDP growth for $L = 512$ at three specific times, $t = 10, 50$, and 100 ML, for three values of $G = D/F$ with $F = 1$. From top to bottom panels, $G = 10, 10^3$, and 10^5.

Surface morphology

Before starting the detailed analysis and the main discussion, we check how the VDP growing surface evolves. In plotting the snapshots of the VDP model growth in figure 2 for various G values at three different stages of the film growth, we observe that the films exhibit tree-like characteristic morphologies and columnar structures with many voids and overhangs for all three cases of G as time elapses. Moreover, as G (the diffusion coefficient) increases, the surface height grows rapidly and the columnar morphology becomes rougher and less dense. In order to work out the origin of the characteristic columnar structure, we investigate the effect of the flux incident angle distribution on the VDP growth. When we fix the monomer incident angle in a single vertical direction such as that of a collimated flux, the surface columnar structures disappear, as shown in figure 3, for all three cases of G. The evolution of surfaces with the VDP model growth is shown in figure 4, where we assume that the surface height is the single value of the highest position at the lateral site. One can see that, as G increases and t elapses, the columnar and grooved structure becomes much clearer.

In section 3, we analyze this unusual VDP growth surface quantitatively with conventional physical quantities in surface growth models as well as polymer properties.

3. Numerical results

We perform numerical simulations with various system sizes up to $L = 1024$ for three values of G, where numerical data are averaged over 100 samples. Unlike the PVD/MBE

J. Stat. Mech. (2009) P02031

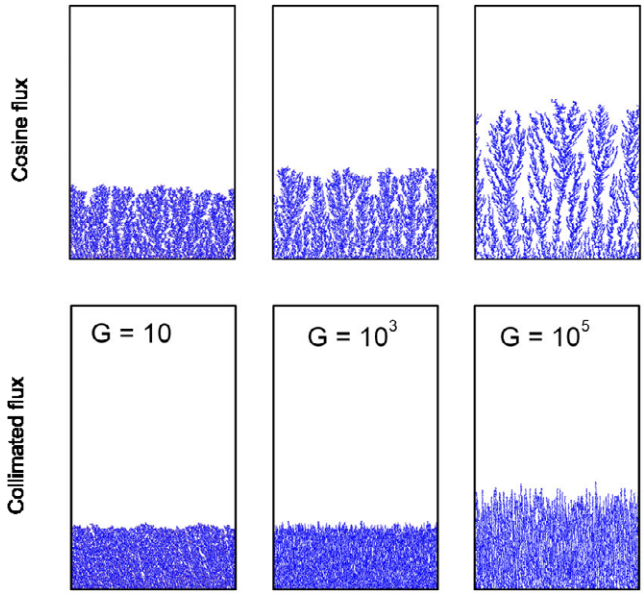

Figure 3. Effect of the flux angle of incidence on the VDP growth model. While the VDP growth with the cosine flux shows the characteristic columnar structures (top panels), such structures disappear when the angle of incidence is set to zero, i.e., for vertically collimated flux (bottom panels). From left to right, $G = 10, 10^3$, and 10^5 for $L = 512$ at $t = 180$ ML.

growth model case, the VDP growth model case requires active end site tracking and polymer indexing, so the largest system size in our MC simulations becomes much smaller than that in ordinary surface growth models.

3.1. Surface roughness and height difference correlation function

We first measure the surface roughness (width) defined as

$$W^2(t) \equiv \langle \overline{[h(x,t) - \bar{h}(t)]^2} \rangle,$$

where $\bar{f}$ is the spatial average, i.e., $\bar{f} = 1/L \sum_x f(x)$, and $\langle \cdots \rangle$ represents the statistical sample average. The width $W(t)$ in the VDP growth for $G = 10$ plotted in figure 5(a), which shows clearly three regimes as L increases: the initial growth, the VDP growth, and the saturation. Unlike the conventional surface growth, the VDP growth exhibits anomalous dynamic scaling, where the VDP growth regime appears after about five monolayers (ML), irrespectively of the system sizes, and it undergoes some unusual behavior before $W(t)$ saturates to $W_{\rm sat}$ due to the finite-size effect. The global dynamic scaling of the VDP surface roughness is governed by the global roughness exponent $\alpha_{\rm global}$, from the system size dependence of the saturated width ($W_{\rm sat} \sim L^{\alpha_{\rm global}}$), and the global dynamic exponent $z_{\rm global}$, from the system size dependence of the saturation time ($t_{\rm sat} \sim L^{z_{\rm global}}$).

In order to investigate the local dynamic scaling of the VDP growth, we also measure the two-point height difference correlation function defined as

$$C_2(r,t) = \langle \overline{|h(x+r,t) - h(x,t)|^2} \rangle,$$

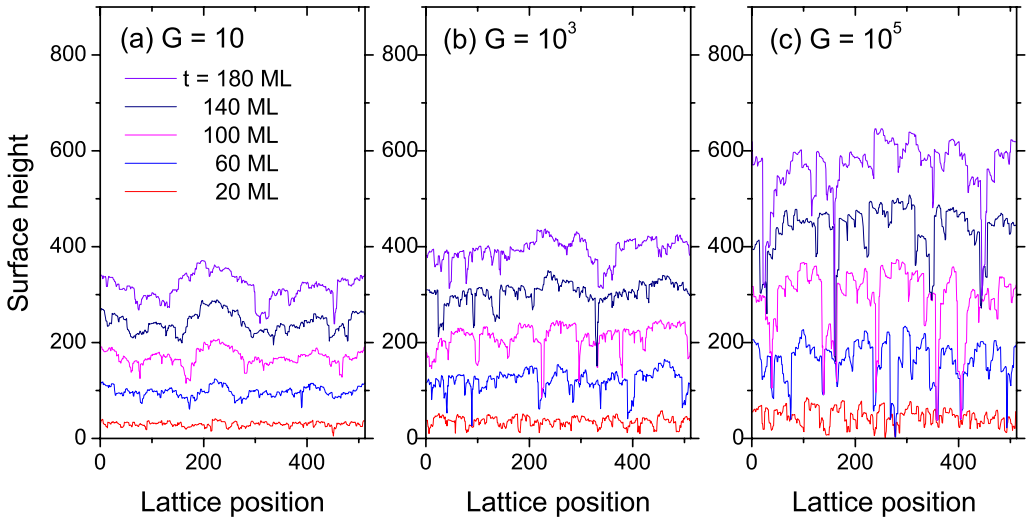

Figure 4. Evolution of surfaces in the VDP growth model. For $L = 512$, (a) $G = 10$, (b) $G = 10^3$, and (c) $G = 10^5$ at $t = 20, 60, 100, 140$ and 180 ML from bottom to top, respectively.

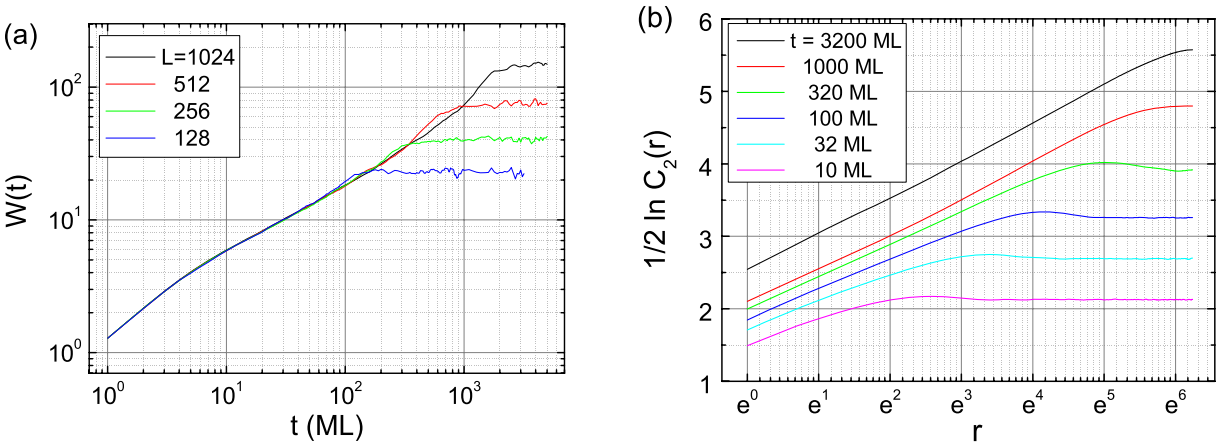

Figure 5. Double-logarithmic plots of W and C_2 for the case of $G = 10$; (a) surface roughness versus time for $L = 128$, 256, 512, and 1024 from bottom to top, and (b) height difference correlation function versus r for $L = 1024$.

which follows $C_2(r,t) \sim r^{2\alpha_{\rm local}}$ for $r < \xi(t)$ and $C_2(r,t) = 2W^2(t)$ for $r > \xi(t)$. Here $\xi(t)$ is the correlation length, scaling as $\xi(t) \sim t^{1/z_{\rm local}}$. Figure 5(b) shows how height correlations and the correlation length are developed at various times for $G = 10$. For three values of G, the global scaling behavior in the VDP growth is compared with the local one. Figure 6 shows clearly that as G increases, the surface becomes rough much faster with larger values of W, and is less dense at each level of the surface height. Moreover, from figures 6(b) and (c), we observe that the initial growth regime gets extended as G increases, while in the real scaling regime for the VDP growth, the effective growth exponents β becomes all the same, as $\beta \simeq 0.5$ ($\neq \alpha_{\rm global}/z_{\rm global}$), irrespectively of the value of G. This implies that at the early stage of the growth, the shadowing effect by the cosine flux is negligible since there are not many polymers, but later on, the shadowing effect governs the surface

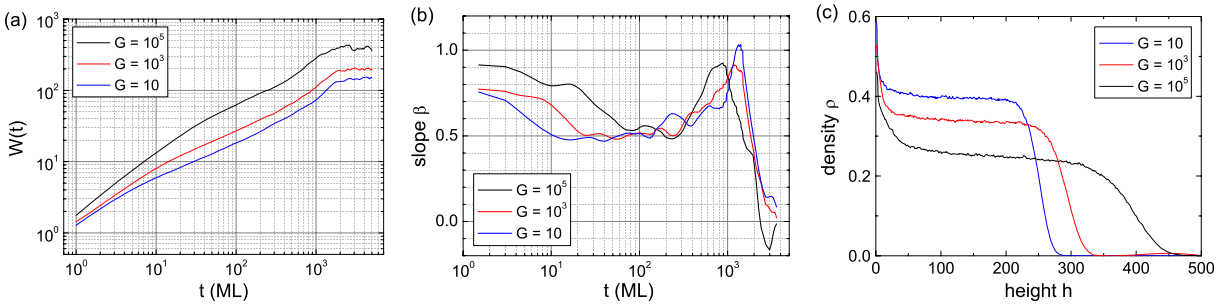

Figure 6. For $L = 1024$, (a) double-logarithmic plots of W against t, (b) semi-logarithmic plots of the effective growth exponent β against t (from bottom to top, $G = 10,\ 10^3$, and 10^5), and (c) the density profile at $t = 100$ ML against surface height h (from top to bottom, $G = 10,\ 10^3$, and 10^5).

Table 1. Summary of roughness exponents and dynamic exponents for various values of G. Unlike the global results, the local results seem to be independent of the G value.

G	$\alpha_{\rm global}$	$\alpha_{\rm local}$	$z_{\rm global}$	$z_{\rm local}$
10	0.89(1)	0.50(2)	1.27(1)	1.27(2)
10^3	0.87(1)	0.47(2)	1.16(1)	1.27(2)
10^5	0.72(1)	0.48(2)	0.81(1)	1.32(2)

growth as well as the active bonding, once polymers form. In the VDP growth regime, the density profile at each height level shows the difference of dynamic processes like a stratum reflects a historical event (see figure 6(c)). Until a polymer forms, the effect of the cosine flux is negligible and the monomer diffusion is dominant, which explains the first decay in the density profile. After the surface height becomes comparable to the characteristic length of a polymer for a given G value, such that there are several structures of polymer lumps, the incident monomer with a certain angle can hang on the other polymer bodies and both the effect of the cosine flux and the diffusion of monomers govern the growth dynamics; this reflects the plateau in the density profile. Finally, the front of the surface is governed by the fluctuations of the locations of active ends, shown as the second decay in the density profile. We wish to note here that the density profile is taken at $t = 100$ ML, which corresponds to the same as the right side panels in figure 2.

Although the qualitative behaviors of the kinetic roughening seem to be similar for the three values of G, its quantitative behavior is quite dependent on the value of G. Such a role of diffusion in the VDP growth is summarized as G-dependent kinetic roughening in table 1, in terms of the roughness exponent, α, and the dynamic exponent, z, for both the global and local cases. It should be noted that the growth exponent β that we found above is different from both $\alpha_{\rm global}/z_{\rm global}$ and $\alpha_{\rm local}/z_{\rm local}$. Therefore, the data for W hardly collapse, due to the VDP growth regime (see figure 7).

3.2. Height and step distributions

In measuring the height distribution, $P(h')$ where $h' = h - \langle h \rangle$, for various times and system sizes, we double-check the anomalous kinetic roughening in our VDP growth model

J. Stat. Mech. (2009) P02031

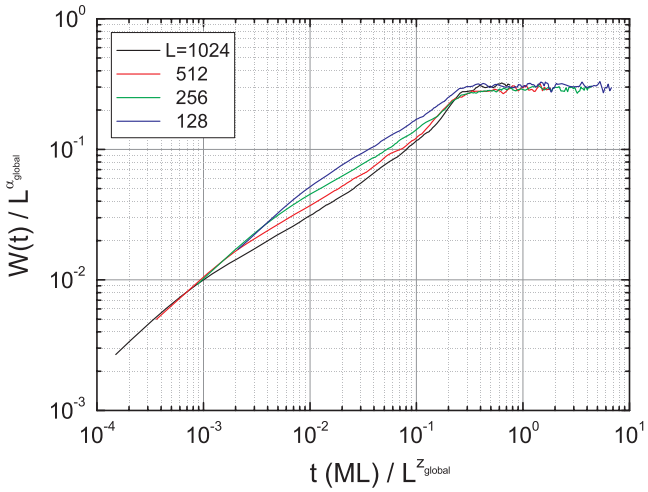

Figure 7. Data collapse of the surface roughness: double-logarithmic plots of $WL^{\alpha_{\rm global}}$ versus $t/L^{z_{\rm global}}$ with $\alpha_{\rm global} = 0.89$ and $z_{\rm global} = 1.27$ for $G = 10$.

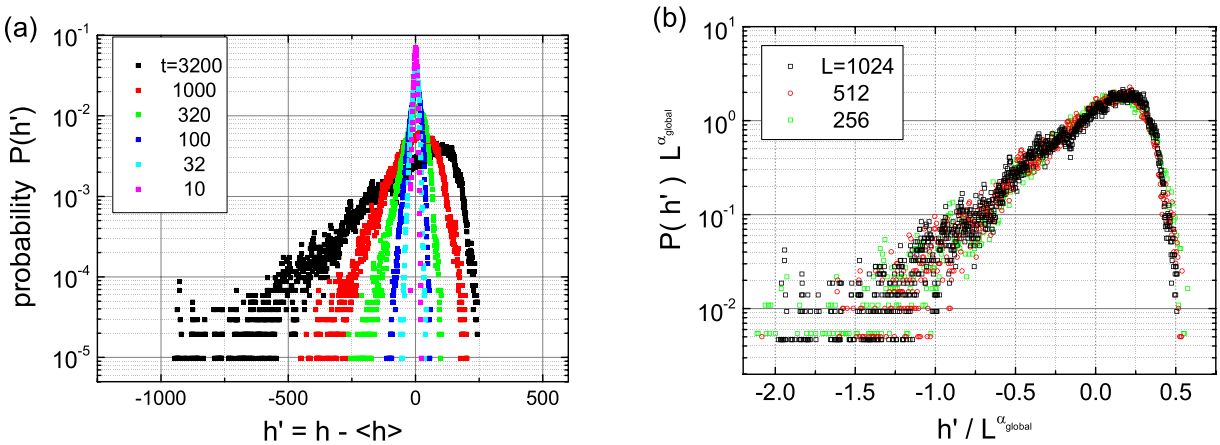

Figure 8. (a) Semi-logarithmic plots of the height distribution function, $P(h')$, against $h' = h - \langle h \rangle$, at various times, $t = 10,\ 32\ ,100,\ 320,\ 1000$, and 3200 ML for $L = 1024$ and $G = 10$. Note that $\langle h \rangle = \bar{h}$ for our case. As t elapses, $P(h')$ becomes broader and is gradually transformed into a right skewed Gaussian distribution. (b) At $t = 3200$ ML, after the surface roughness gets saturated, $P(h')$ exhibits scaling behavior with $\alpha_{\rm global}$, which is confirmed for various system sizes $L = 256,\ 512$, and 1024, as $P(h')L^{\alpha_{\rm global}}$ versus $h'/L^{\alpha_{\rm global}}$ with $\alpha_{\rm global} = 0.89$ for $G = 10$.

and also confirm our numerical finding of $\alpha_{\rm global}$ by collapsing the data (see figure 8) for $P(h')$. The height distribution becomes broader as time elapses, which means that the surface gets rougher for larger values of the width W since W corresponds to the standard deviation of $P(h')$. At the initial stage, $P(h')$ is almost Gaussian and symmetric, while at the final stage, the distribution is slightly skewed to the right, where the exponential decay tail below the average height (left) is broader than that above it (right).

It is observed that the anomalous kinetic roughening in the VDP growth is attributable to the power-law distribution of the height difference among the nearest

doi:10.1088/1742-5468/2009/02/P02031

J. Stat. Mech. (2009) P02031

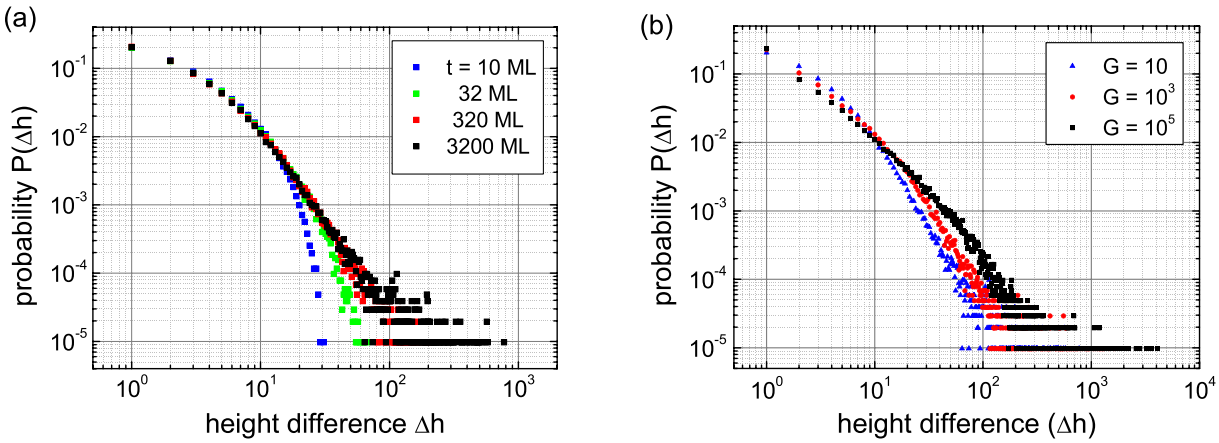

Figure 9. Power-law step distributions for $L = 1024$: (a) at various times only for $G = 10$ and (b) for three values of G only at $t = 3200$ ML.

neighboring sites, i.e., $r = 1$ (namely a 'step'), for $P(\Delta h)$, which implies that the VDP growth exhibits multifractality as well as $\alpha_{\text{global}} \neq \alpha_{\text{local}}$. We investigate how the power-law behavior of $P(\Delta h)$ changes as t elapses and as G increases. Figure 9 shows that for the larger values of Δh the decay exponent seems to be independent of the G value in the steady-state limit. It is very interesting that the step distribution shows clearly a power-law decay for large values Δh ($\equiv |h(x+1) - h(x)|$) after W gets saturated.

This is somewhat similar to the case for the ballistic deposition model with a power-law noise [10]. In that sense, we suspect that the active ends play a crucial role in the power-law step distribution, the details of which are under investigation [11].

3.3. Polymer properties

In the VDP growth, the properties of the polymer are also important (to be discussed). After measuring the time-dependent frequency of the polymers per site, $D(L_{\text{p}})$, where L_{p} is the length of polymer for $L = 1024$, as well as the end-to-end distances (see figure 10), we finally investigate such properties. As time elapses, monomers are deposited on the surface more and more, so the number of polymers increases and at the same time polymers get longer. On the basis of our numerical finding, there is a typical length scale of polymers for a given value of G in the steady state of the VDP growth. It is observed that the typical length of a polymer gets longer as G increases (see figure 10(b)). For example, one typical polymer consists of about 15 monomers at $G = 10$, while it consists of 434 monomers at $G = 10^5$. Figure 10(c) shows that the root mean square of the end-to-end distance for a given polymer, $\langle R^2_{\text{e-e}} \rangle^{1/2}$, scales as $\langle R^2_{\text{e-e}} \rangle^{1/2} \propto L^{\nu}_{\text{p}}$, where we find that the exponent ν is about 0.75 for short polymers under about 100 monomers in length, but 1.0 for long polymers. Therefore, as G increases, it is observed that a crossover from $\nu = 0.75$ to 1 occurs. Here, the exponent ν represents the inverse of the fractal dimension of the polymers. One can say that $D_{\text{f}} = 1.33$ at $G = 10$, which is the same as the value for linear polymers formed by self-avoiding walks [2]. The detailed analysis has been investigated [11].

J. Stat. Mech. (2009) P02031

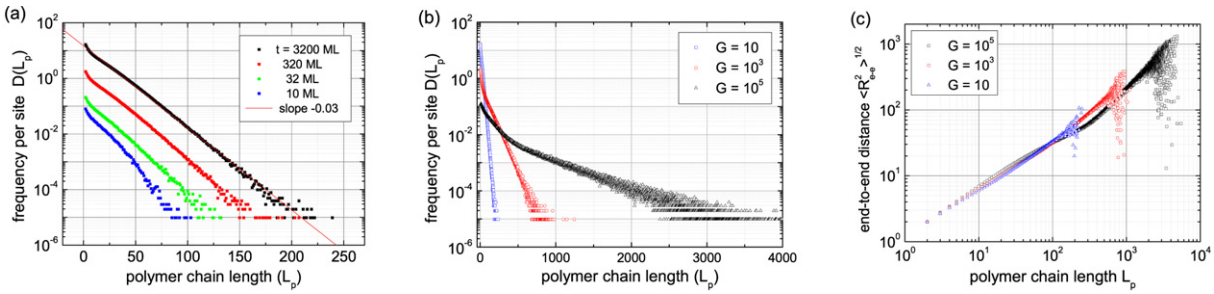

Figure 10. Semi-logarithmic plots of the polymer chain length distribution $D(L_\mathrm{p})$ against the length of polymer L_p (a) for $G = 10$ at various times and (b) for various G values at $t = 3200$ ML, where $L = 1024$. For the same setup as (b), (c) shows double-logarithmic plots of the end-to-end distance of the polymer, $\langle R^2_{\mathrm{e-e}}\rangle^{1/2}$, against L_p.

3.4. Growth of $(2+1)$-dimensional VDP thin films

The $(2+1)$-dimensional version of our model has also been considered in order to explain the most recent experimental results obtained by Lee and co-workers [6]; the growth of PPX-C films was discussed by the same authors. It is noted that our extended version can be considered as a modification of the earlier study by Zhao and co-workers [12] for the VDP process in the submonolayer regime. In our extension, multilayer growth is allowed, with the coalescence process of polymers. Our preliminary results for a $(2+1)$-dimensional lattice [13] seem to be quite different from those for a $(1+1)$-dimensional lattice, but they also exhibit anomalous scaling behavior in kinetic roughening with multifractality; this is similar to the experimental results, except that the valley filling regime seems to be missing in our model study. To answer the question of the origin of the valley filling regime of the experimental results, it might be necessary that we also consider some new dynamics, such as the chain relaxations that we ignored in our current version. Considering polymer properties in the VDP growth would be another key to identifying the universality class of the VDP growth more clearly. For example, we suspect that reptation with zigzag paths governs the sublinear scaling behavior at early stages of the polymer growth, while the polymer interactions become relevant after polymers grow enough to be comparable with the typical length, so the coalescence of polymers allows them to show linear scaling, as shown in the $(1+1)$-dimensional version. Such properties have also been investigated in our modified version for a $(2+1)$-dimensional lattice [13].

4. Summary and remarks

In summary, we studied a simple toy model for the growth of polymer thin films by vapor deposition polymerization (VDP) processes in order to explain recent experimental results on the coating processes of poly(p-xylylene) (PPX) and its derivatives, e.g., PPX-C. It is found that the VDP growth is quite different from the conventional molecular beam epitaxy (MBE) growth for the growth of metal or semiconductor films. In particular, we argued that anomalous scaling behavior in kinetic roughening for the VDP growth is attributable to the instability induced by the non-local shadowing effects as well as active

bonding in polymerization. As further clear evidence of such anomalies, we showed power-law step distributions, directly related to the multifractality of the VDP growth. The two-point height difference qth-moment analyses are also under detailed investigation [11, 13].

Finally, we would like to comment on polymer interaction, i.e., the coalescence process of polymers, which is the new aspect of our model. In earlier studies, polymer interactions and chain relaxation are often omitted from dynamic rules due to their complexity in model simulation codes. We retained polymer interactions since they play a crucial role in the comparison with real experimental data, in particular for the polymer structure and its growth, while we also omitted the chain relaxation rule for the same reason. In the model without polymer interaction studied by Bowie and Zhao [8], the number of active ends of polymers always increases, since there is no mechanism for reducing the number of polymers, while in our model, the incrementation of polymers slows down as polymers are merged into others. One polymer interaction removes two active ends, and the active ends are the stabilizing sites of monomers in the VDP growth model. Thus, one can readily anticipate that the monomers in our model are more abundant as compared to the case for excluding the coalescence process. Moreover, the diffusion probability $P_{\mathrm{D}} = G\rho_{\mathrm{m}}/(G\rho_{\mathrm{m}} + 1)$ can effectively increase when the ratio of the diffusion rate to the deposition flux rate G is compatible with the monomer density ρ_{m}. Of course, such an effect becomes negligible when $G \gg \rho_{\mathrm{m}}$ since the number of polymers is small, so the polymer coalescence process rarely happens. Regarding the effects of the coalescence of polymers on the polymer structure and its growth in our model, we have observed that in the characteristic polymer, the length definitely becomes greater and the fractal dimension of polymers clearly gets larger from $D_{\mathrm{f}} = 1.08$ to 1.33 (closer to that of self-avoiding walk polymers), as compared to the case of excluding polymer interaction [8, 11]. In contrast to the dramatic polymer structural change, the surface roughnesses behave in almost the same way in the two cases even though the number of monomers in our model rapidly increases as compared to the case when excluding polymer interaction, as expected. Therefore, we conclude that the polymer interaction mechanism gives us a better understanding of the polymer structural properties than its growth properties in the $(1 + 1)$-dimensional case. The role of such a mechanism in the $(2 + 1)$-dimensional case will be discussed elsewhere [13].

Acknowledgments

This work was supported by the BK21 project (MH) and Acceleration Research (CNRC) of MOST/KOSEF through the grant No. R17-2007-073-01001-0 (SS) and by the Korean Systems Biology Program from MEST through KOSEF (No. M10309020000-03B5002-00000, HJ). We would like to acknowledge fruitful discussions with I J Lee, who gave us the main idea for this work and let it be initiated, and valuable comments from J Krug and J M Kim.

References

[1] Family F and Vicsek T (ed), 1991 *Dynamics of Fractal Surfaces* (Singapore: World Scientific)
Barabási A-L and Stanley H E, 1995 *Fractal Concepts in Surface Growth* (Cambridge: Cambridge University Press)
[2] Meakin P, 1998 *Fractals, Scaling and Growth far from Equilibrium* (Cambridge: Cambridge University Press)
[3] Wong C P (ed), 1993 *Polymers for Electronic and Photonic Applicants* (Boston, MA: Academic)

J. Stat. Mech. (2009) P02031

[4] Collins G W, Letts S A, Fearon E M, McEachern R L and Bernat T P, 1994 *Phys. Rev. Lett.* **73** 708
Biscarini F, Samorí P, Greco O and Zamboni R, 1997 *Phys. Rev. Lett.* **78** 2389
[5] Zhao Y-P, Fortin J B, Bonvallet G, Wang G-C and Lu T-M, 2000 *Phys. Rev. Lett.* **85** 3229
Punyindu P and Das Sarma S, 2001 *Phys. Rev. Lett.* **86** 2696
Zhao Y-P, Fortin J B, Bonvallet G, Wang G-C and Lu T-M, 2001 *Phys. Rev. Lett.* **86** 2697
[6] Lee I J, Yun M, Lee S-M and Kim J-Y, 2008 *Phys. Rev.* B **78** 115427
[7] Beach W F, 1977 *Macromolecules* **11** 72
Beach W F, Lee C, Basset D R, Austin T M and Olson O, 1989 *Encyclopedia of Polymer Science and Engineering* 2nd edn, vol 7 (New York: Wiley) p 990
[8] Bowie W and Zhao Y-P, 2004 *Surf. Sci.* **563** L245
Zhao Y-P and Bowie W, 2005 *Mater. Res. Soc. Symp. Proc.* E **859** JJ6.4.1
[9] Drotar J T, Zhao Y-P, Lu T-M and Wang G-C, 2000 *Phys. Rev.* B **62** 2118
Karabacak T, Zhao Y-P, Wang G-C and Lu T-M, 2001 *Phys. Rev.* B **64** 085323
Yang Y G, Hass D D and Wadley H N G, 2004 *Thin Solid Films* **471** 1
Yanguas-Gil A, Cotrino J, Barranco A and González-Elipe A R, 2006 *Phys. Rev. Lett.* **96** 236101
Pelliccione M, Karabacak T and Lu T-M, 2006 *Phys. Rev. Lett.* **96** 146105
Pelliccione M, Karabacak T, Gaire C, Wang G-C and Lu T-M, 2006 *Phys. Rev.* B **74** 125420
[10] Zhang Y-C, 1990 *Physica* A **170** 1
Krug J, 1991 *J. Physique* **1** 9
Buldyrev S V, Havlin S, Kertesz J, Stanley H E and Vicsek T, 1991 *Phys. Rev.* A **43** 7113
Lam C-H and Sander L M, 1992 *Phys. Rev. Lett.* **69** 3338
Lam C-H and Sander L M, 1992 *J. Phys. A: Math. Gen.* **25** L135
Lam C-H and Sander L M, 1993 *Phys. Rev.* E **48** 979
Barabási A-L, Bourbonnais R, Jensen M, Kertesz J, Vicsek T and Zhang Y-C, 1992 *Phys. Rev.* A **45** R6951
[11] Son S-W, Ha M, Jeong H and Lee I J, 2009 in preparation
[12] Zhao Y-P, Hopper A R, Wang G-C and Lu T M, 1999 *Phys. Rev.* E **60** 4310
Zhao Y-P, Hopper A R, Wang G-C and Lu T M, 2000 *Phys. Rev.* E **61** 2156
[13] Son S-W, Ha M, Lee I J and Jeong H, 2008 unpublished data

J. Stat. Mech. (2009) P02031